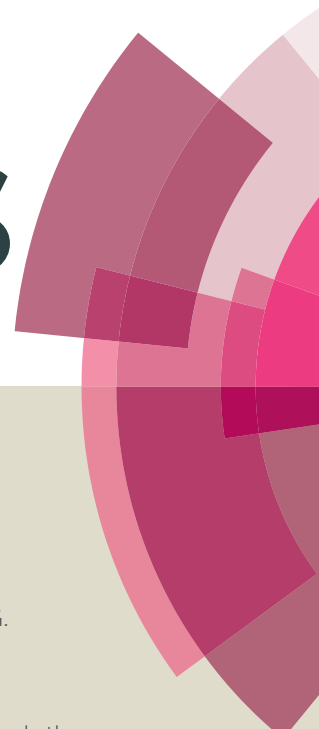


RSC Advances



This article can be cited before page numbers have been issued, to do this please use: B. A. D. Neto, G. Dias, P. Pinho, H. A. Duarte, J. M. Resende, A. Rosa, J. Corrêa and E. Silva Junior, *RSC Adv.*, 2016, DOI: 10.1039/C6RA14701A.



This is an *Accepted Manuscript*, which has been through the Royal Society of Chemistry peer review process and has been accepted for publication.

Accepted Manuscripts are published online shortly after acceptance, before technical editing, formatting and proof reading. Using this free service, authors can make their results available to the community, in citable form, before we publish the edited article. This *Accepted Manuscript* will be replaced by the edited, formatted and paginated article as soon as this is available.

You can find more information about *Accepted Manuscripts* in the [Information for Authors](#).

Please note that technical editing may introduce minor changes to the text and/or graphics, which may alter content. The journal's standard [Terms & Conditions](#) and the [Ethical guidelines](#) still apply. In no event shall the Royal Society of Chemistry be held responsible for any errors or omissions in this *Accepted Manuscript* or any consequences arising from the use of any information it contains.

Fluorescent Oxazoles from Quinones for Bioimaging Applications

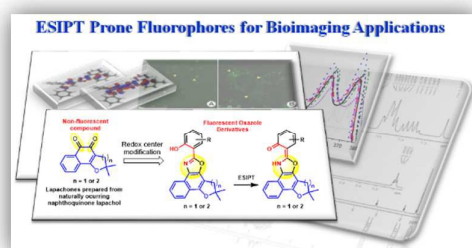
Gleiston G. Dias,^a Pamela V. B. Pinho,^a Hélio A. Duarte,^a Jarbas M. Resende,^a Andressa B. B. Rosa,^b

José R. Correa,^b Brenno A. D. Neto^{b*} and Eufrânio N. da Silva Júnior^{a*}

^a Institute of Exact Sciences, Department of Chemistry, Federal University of Minas Gerais, Belo Horizonte, 31270-901, MG, Brazil. E-mail: eufranio@ufmg.br

^b Laboratory of Medicinal & Technological Chemistry, Institute of Chemistry, University of Brasilia, P.O. Box 4478, Brasilia, 70904970, DF, Brazil. E-mail: brenno.ipi@gmail.com

Table of Contents Graphic

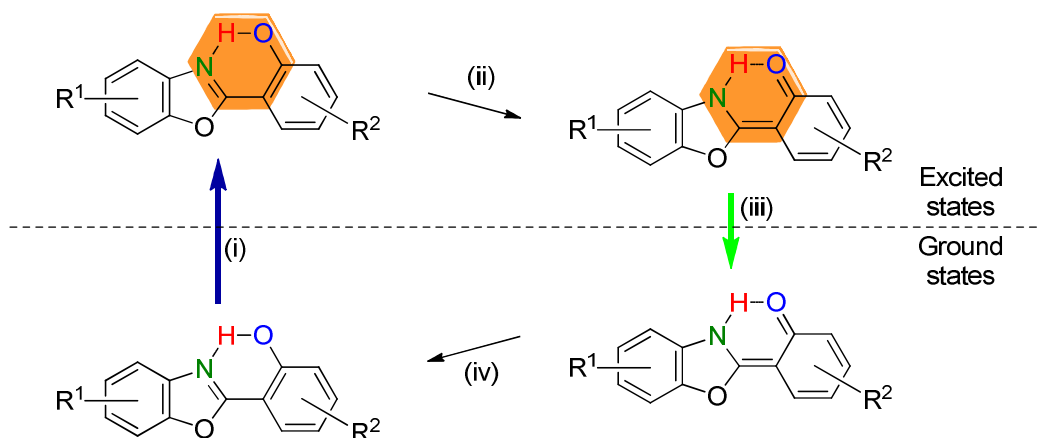


Abstract. This work describes a synthetic strategy for the syntheses of four new fluorescent excited state intramolecular proton transfer (ES IPT) prone oxazole derivatives synthesized from lapachol, a naturally occurring naphthoquinone isolated from *Tabebuia* species (ipe tree). DFT calculations were performed to understand the ES IPT stabilizing process of these new derivatives. The new structures were designed to have improved lipophilic and balanced hydrophobic properties toward a selective cellular staining of lipid-based structures, that is, lipid inclusions in the cytosol. Cell-imaging experiments returned interesting results and showed the molecular architecture of the four derivatives had a great influence over the stabilizing processes in the excited state and over the selection of lipid inclusions inside the cells.

INTRODUCTION

The development of new, designed and more efficient bioprobes is a hard and challenge task.¹ Whether one consider the new probes must meet strict requirements of chemical- and photostabilities associated with specific responses inside the astonishing cellular environment, than this task is even more puzzling.²⁻⁴ Most of the available cellular probes used for bioimaging applications, especially commercially available structures, have been built over a few 'classical' scaffolds i.e. coumarins, boron-dipyrromethenes (BODIPYs), rhodamines, cyanines, phenoxazines and fluoresceins. The great advances and drawbacks associated with these fluorescent derivatives have been reviewed elsewhere.⁵ Although derivatives synthesized from these scaffolds are commonly used for the development of bioprobes,⁶ many alternatives are emerging aiming to succeed where those derivatives have already shown their limitations and drawbacks, as some of us recently highlighted.⁷ Among the available alternatives, fluorescent derivatives bearing a unit of benzothiadiazole,^{8,9} benzothiazole,^{10,11} benzimidazole,^{12,13} imidazopyridine,^{14,15} and oxazole^{16,17} are some promising structures to further bioprobes technology.

Oxazole derivatives are a very attractive class of heterocycles prone to perform ES IPT (excited-state intramolecular proton transfer) stabilizing processes (Scheme 1).¹⁸⁻²¹ These derivatives may be used in many light technological areas and have been applied as fluorescent tags for multicomponent adducts,²² white emitters,²³ probes for model membranes,²⁴ metal sensors²⁵ and others.²⁶ Although oxazole derivatives are a promising class of fluorescent heterocycles, the rational design towards cellular selectivity in bioimaging experiments is a gap not fulfilled hitherto.



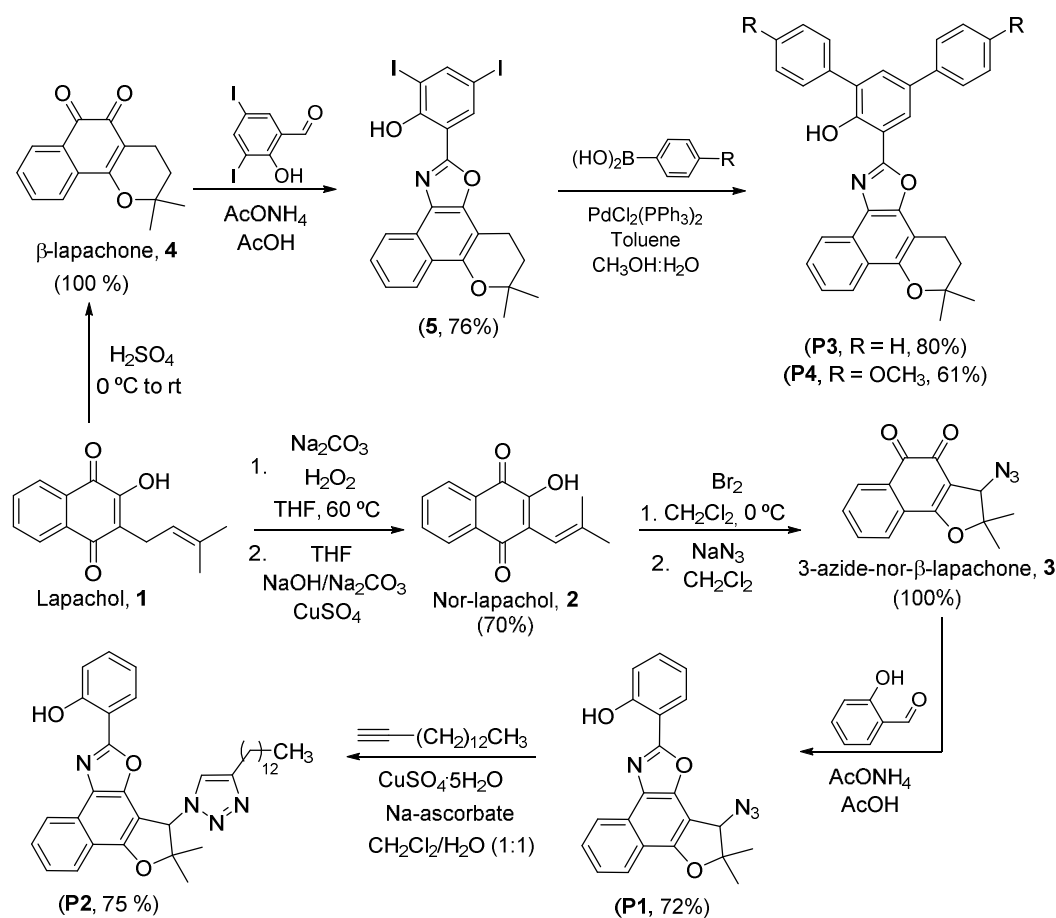
Scheme 1. General structure of an ESIPT prone oxazole derivative and its excited-state intramolecular proton transfer mechanism. (i) Absorption, (ii) proton transfer in the excited state, (iii) emission and (iv) reverse proton transfer.

Because of our interest in the development new fluorescent probes for bioimaging applications,²⁷⁻³² we disclose herein the syntheses of four new fluorescent oxazole derivatives, their molecular architecture designed for targeting lipophilic structures (lipids inclusions) inside the cells, their photophysical and theoretical (DFT) evaluations and their bioimaging applications.

RESULTS AND DISCUSSION

The new fluorescent derivatives were synthesized as shown in Scheme 2. The synthetic strategy was based on the redox center modification of β -lapachone and nor- β -lapachone derivatives prepared from the natural occurring lapachol (**1**), a quinone derivative easily obtained from ipe tree.³³⁻³⁶ We have successfully used this sort of strategy towards the synthesis of boron-based structures applied as superior probes for endocytic pathway tracking in live cancer cells²⁹ and selective fluorescent sensor for cadmium ions.³⁷ Lapachol (**1**) could be directed converted to nor-lapachol (**2**) by the well-established Hooker oxidation method³⁸ and then transformed in the key

intermediate 3-azide-nor- β -lapachone (**3**). Exploring the electrophilicity of the *ortho*-quinoidal carbonyls of the respective azide derivative by the reaction with salicylaldehyde in the presence of a nitrogen source the oxazole **P1** was prepared.³⁹ The click reaction⁴⁰⁻⁴² of **P1** afforded **P2** bearing a long side carbon chain. Lapachol (**1**) was also used to obtain β -lapachone (**2**) which in turn was used to the synthesis of the iodinated oxazole (**5**). Key iodinated intermediate (**5**) directly afforded **P3** and **P4** through the Suzuki reaction.

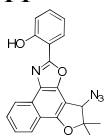
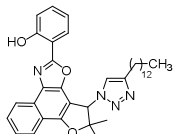
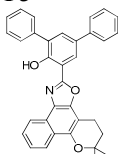
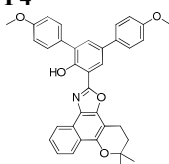


Scheme 2. Synthesis of fluorescent oxazole derivatives named **P1-P4**.

Derivative **P1-P4** had their photophysical evaluated and results are summarized in Table 1 (also see Figures S41-43 in the Supporting Information file). **P1-P2** showed small Stokes shifts and reasonable molar extinction coefficients with $\log \epsilon$ values in the

range of 3.41-3.66 $\text{mM}^{-1} \text{cm}^{-1}$. These data indicate the ESIPT were not as efficient as expected to be. **P3** and **P4** however showed a very distinct behavior. It could be noted (for **P3** and **P4**) large Stokes shifts (141-184 nm) and large molar extinction coefficients (log ϵ values in the range of 4.08-4.39 $\text{mM}^{-1} \text{cm}^{-1}$). ESIPT prone fluorophores typically have large Stokes shift and this feature is known to be a spectroscopic signature of the efficient process.⁴³ Some theoretical calculations have been performed to a better understand of the photophysical related to the synthesized compounds, as show in Figure 1.

Table 1. Photophysical data (in different solvents) for **P1-P4** (10 μM solutions for all analyses).

Oxazole	Solvent	λ_{max} (abs) (nm)	log ϵ (ϵ)	λ_{max} (em) (nm)	Stokes Shift (nm)
P1 	ethyl acetate	370	3.57 (3736)	398	28
	acetonitrile	369	3.52 (3344)	400	31
	dichloromethane	372	3.57 (3708)	400	28
	dimethyl sulfoxide	374	3.57 (3708)	404	30
	hexane	369	3.66 (4530)	395	26
	methanol	369	3.56 (3671)	396	27
	toluene	374	3.59 (3868)	401	27
P2 	ethyl acetate	369	3.51 (3225)	396	27
	acetonitrile	369	3.51 (3208)	397	28
	dichloromethane	371	3.54 (3482)	399	28
	dimethyl sulfoxide	373	3.41 (2574)	403	30
	hexane	368	3.64 (4365)	393	25
	methanol	368	3.52 (3305)	395	27
	toluene	372	3.58 (3781)	398	26
P3 	ethyl acetate	378	4.28 (19068)	528	150
	acetonitrile	377	4.32 (21032)	525	148
	dichloromethane	380	4.31 (20432)	521	141
	dimethyl sulfoxide	381	4.32 (20736)	534	153
	hexane	378	4.39 (24436)	531	153
	methanol	377	4.22 (16652)	521	144
	toluene	383	4.33 (21606)	528	145
P4 	ethyl acetate	363	4.30 (19726)	540	177
	acetonitrile	363	4.30 (19962)	541	178
	dichloromethane	365	4.33 (21572)	540	175
	dimethyl sulfoxide	367	4.26 (18276)	551	184
	hexane	360	4.34 (21740)	539	179
	methanol	363	4.08 (12090)	540	177
	toluene	366	4.26 (18284)	541	175

Quantum yields (in dichloromethane) for **P1-P4** of 0.70, 0.45, 0.55, and 0.51, respectively.

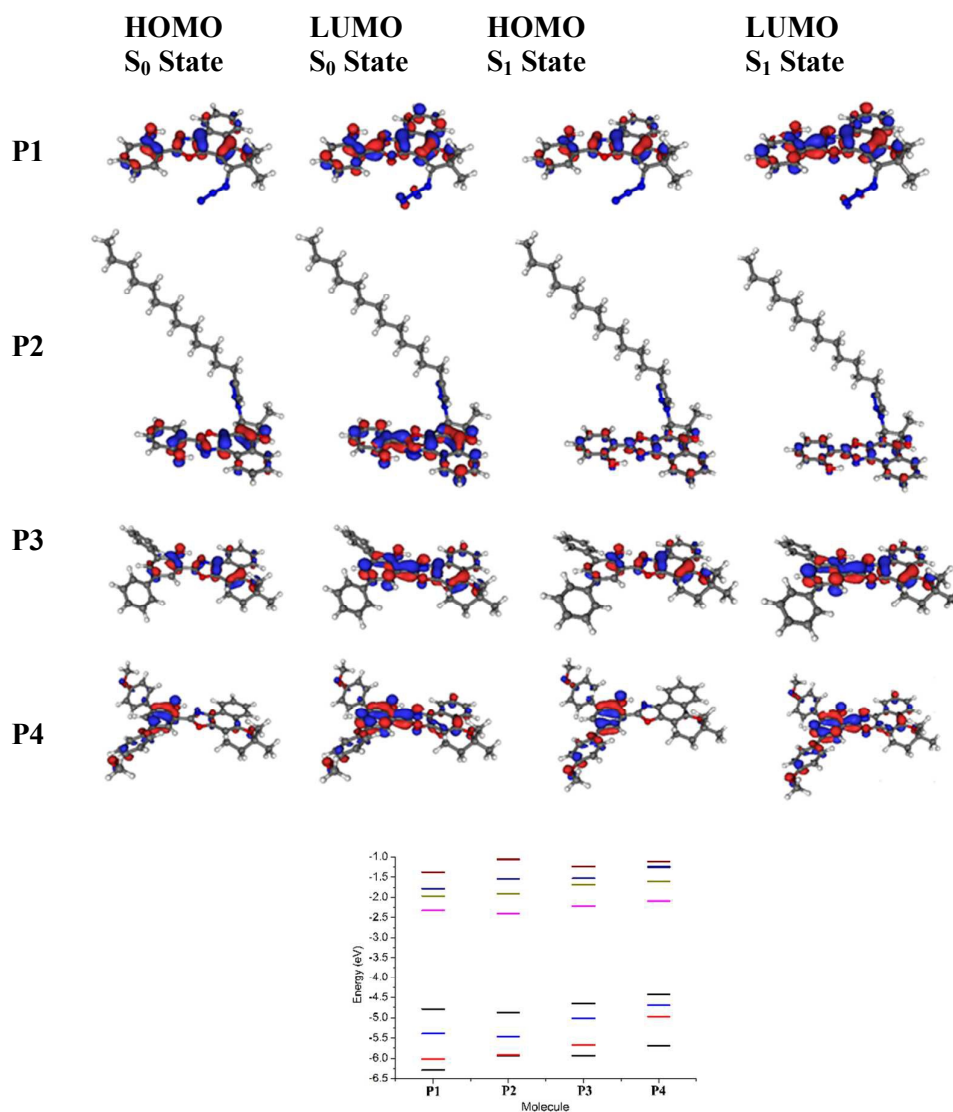


Figure 1. HOMO and LUMO plots and diagram of the frontier molecular orbital energies. Calculations performed at the PBEPBE/cc-pVDZ level of theory.

It is noted in both the ground and excited states the LUMO orbitals of **P3-P4** are centered in the oxazole ring whereas for **P1-P2** the same orbitals are more distributed in the structures. These results allow to a better understanding on the efficiency of the H-transfer in the excited state (ESIPT) for **P3-P4** and the large Stokes shifts obtained in the photophysical experiments.

Finally, compounds **P1-P4** had their capacity as bioimaging probes tested against Caco-2 (human colorectal adenocarcinoma cells) cells lineage (Figure 2). All compounds could be visualized at the green channel bearing a strong fluorescence emission. Their lipophilic nature feature could be beneficially used in the experiments toward lipid inclusions staining.

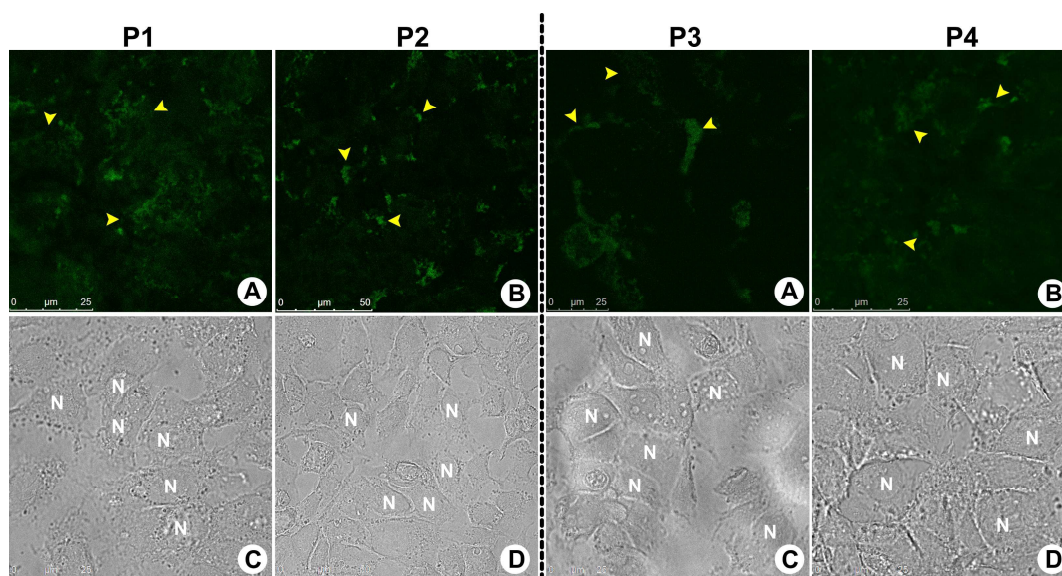


Figure 2. (Left) Fixed caco-2 cell lineages stained with **P1-P2** (10 μ M). (A) and (B) Fluorescence pattern of **P1** and **P2** (respectively) showing a disperse emission in the cytosol but with an accumulation near the peripheral regions of the cells (yellow arrow heads). These feature was more pronounced using **P2** and the tendency toward lipid droplets (vesicles) could be clearer noted. (C) and (D) show the normal morphological aspects of the samples by phase. (Right) Fixed caco-2 cell lineages stained with **P3-P4** (10 μ M). (A) and (B) Fluorescence pattern of **P3** and **P4** (respectively) showing a disperse emission in the cytosol for **P3** but with clear accumulation in the lipid inclusions for **P4** (yellow arrow heads). (C) and (D) show the normal morphological aspects of the samples by phase. N = nucleus and scale bar of 25 μ M.

Compounds **P1-P2** displayed only the so-called minimum selection and were found in the cells' cytosol but not inside the nuclei. **P1** was completely dispersed in the cytosol whereas compound **P2** showed a tendency toward lipid droplets but it was also dispersed in the cytosol (leakage), therefore not suitable as a probe for analyzing these

lipid inclusions. This tendency could be attributed to the long side carbon chain noted in **P2** structure obtained from the azide in **P1**. In order to improve this tendency, we considered the substitution of the carbon chain for lipophilic and hydrophobic groups (e.g. aromatic groups) and, in this sense, compounds **P3** and **P4** were synthesized. **P3** did not show the expected behavior and it was found mostly dispersed in the cytosol as **P1**. Only a tendency for lipids inclusions could be noted using **P3**. **P4** showed however a better accumulation in the lipid bodies than the three previously tested compounds. Theoretical $\log P$ (c $\log P$) values were calculated using DFT and semi-empirical levels (Table S6). The data corroborated the experimental observations and values of lipophilicity for **P4** larger than those observed for **P1-P3** were obtained. Commercial BODIPY was then used to compare and confirm the preference for lipid droplets of compound **P4** and this feature could be therefore confirmed (Figure 3 and Figure S56).

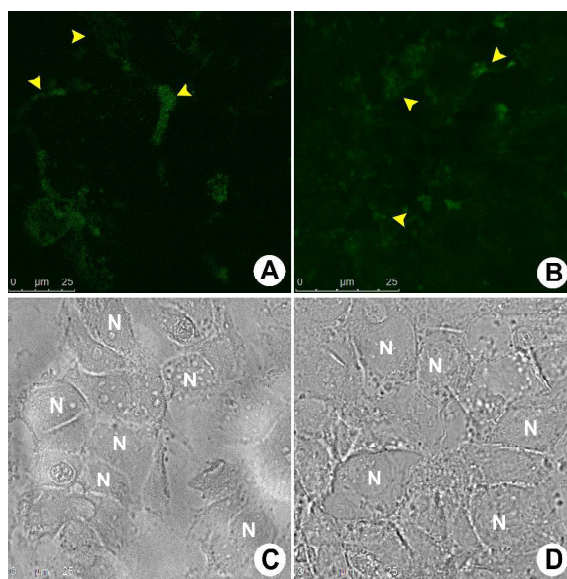


Figure 3. Fixed caco-2 cell lineages stained with **P4** (10 μ M) and commercial available BODIPY. (A) Cells stained with **P4** showing its accumulation in the lipid droplets (yellow arrowheads) and some part still dispersed in the cytosol. (B) Lipid droplets stained with BODIPY. (C) and (D) show the normal morphological aspects of the samples by phase. N = nucleus and scale bar of 25 μ M.

Figure 3-A shows the lipid droplets being gradually stained with **P4**. Even using the commercially available dye for lipid droplets (Figure 3-B), still some part of the dye was noted dispersed in the cytosol, especially considering fixed cells are being used. The selectivity noted for **P4** may be attributed to its higher hydrophobic character indicating the rationale of its synthesis may be applied for further developments of new oxazole-based bioprobes. During the experiment time period no notable photobleaching or degradation could be observed for these dyes thus indicating the chemical- and photo- stabilities are sustained inside the cells, in accordance with the photostability experiment (Figure S57). Commercial BODIPY is known to suffer from photobleaching and this feature limits long time period experiments. The obtained results for **P4** are the first (to the best of our knowledge) toward a clear cellular selectivity of designed oxazoles from natural products therefore this work may be the bases for the development of other fluorescent oxazole derivatives from several classes of natural products, especially quinones.

CONCLUSIONS

For new fluorescent oxazole derivatives have been obtained from the natural product lapachol using an efficient synthetic methodology. Two of these derivatives (**P3-P4**) prove to perform efficient ESIPT whereas the other two did not show the expected behavior in the excited state, although they proved to be stable emitters. DFT calculations allowed for a better understanding on the efficiency of the ESIPT processes

of **P3-P4** and the LUMO orbitals were most centered in the oxazole ring. **P1-P4** had their abilities as bioprobes tested against caco-2 cell lineages. **P1-P2** returned poor results whereas **P3** showed a tendency to accumulate in lipid inclusions. **P4** however proved to be the most selective fluorescent oxazole tested in this work and its molecular architecture may be used as the base for the development of new stable and selective emitters for bioimaging applications. Finally, it is important to add that although a huge progress is observed with these new designed oxazole derivatives, much is yet necessary to establish them as a new class of bioprobes and we are on the way to reach this goal.

EXPERIMENTAL SECTION

General. Melting points were obtained on Thomas Hoover and are uncorrected. Analytical grade solvents were used. Column chromatography was performed on silica gel (SiliaFlash G60 UltraPure 60-200 μm , 60 \AA). Infrared spectra were recorded on an FTIR Spectrometer IR Prestige-21 Shimadzu. ^1H and ^{13}C NMR spectra were recorded at 303 K using a Bruker AVANCE DRX400 spectrometer. All samples for NMR were prepared in CDCl_3 containing TMS as internal reference. Chemical shifts (δ) are given in ppm and coupling constants (J) in Hertz. High resolution mass spectra (electrospray ionization) were obtained using a MicroTOF Ic – Bruker Daltonics instrument.

Chemistry. Lapachol (**1**) was initially extracted from the heartwood of *Tabebuia* sp. (*Tecoma*) and purified by a series of recrystallizations. Initially, nor-lapachol (**2**) was synthesized by Hooker oxidation methodology³³ and data are consistent with those reported in the literature.⁴⁴⁻⁴⁶ Compound **2** was obtained as an orange solid (160 mg, 0.7 mmol, 70% yield); m.p. 121-122 $^\circ\text{C}$.³³ ^1H NMR (400 MHz, CDCl_3 , 303 K) δ : 8.13 (ddd, 1H, $J = 7.5, 1.5$ and 0.5 Hz), 8.10 (ddd, 1H, $J = 7.5, 1.5$ and 0.5 Hz), 7.76 (td, 1H, $J =$

7.5, 7.5 and 1.5 Hz), 7.69 (td, 1H, $J = 7.5, 7.5$ and 1.5 Hz), 6.03-5.99 (m, 1H), 2.0 (d, 3H, $J = 1.5$ Hz), 1.68 (d, 3H, $J = 1.2$ Hz). ^{13}C NMR (100 MHz, CDCl_3 , 303 K) δ : 184.7, 181.5, 151.1, 143.6, 134.9, 133.0, 132.9, 129.5, 126.9, 126.0, 120.9, 113.6, 26.5, 21.7.

Synthesis of 3-azido-2,2-dimethyl-2,3-dihydronaphtho[1,2-*b*]furan-4,5-dione

(3): To a solution of nor-lapachol (**2**) (228 mg, 1.0 mmol) in 25 mL of chloroform, 2 mL of bromine was added. The bromo intermediate precipitated immediately as an orange solid. After removal of bromine, by adding dichloromethane and then removing the organic solvent with dissolved bromine by rotary evaporator, an excess of sodium azide (2 mmol) was added in CH_2Cl_2 and the mixture was stirred overnight. The crude reaction mixture was poured into 50 mL of water. The organic phase was extracted with organic solvent, dried over sodium sulfate, filtered, and evaporated under reduced pressure. The product **3** was obtained after recrystallization as an orange solid (263 mg, 0.98 mmol, 98% yield); m.p. 200-202 °C. ^1H NMR (400 MHz, CDCl_3 , 303 K) δ : 8.14 (ddd, 1H, $J = 6.9, 2.1$ and 0.9 Hz), 7.72-7.65 (3H, m), 4.77 (1H, s), 1.67 (3H, s), 1.55 (3H, s). ^{13}C NMR (100 MHz, CDCl_3 , 303 K) δ : 180.3, 175.2, 170.2, 134.5, 132.7, 131.1, 113.5, 129.5, 125.1, 126.7, 95.5, 67.3, 27.1, 21.9. Data are consistent with those reported in the literature.⁴⁷

General procedure for the synthesis of β -lapachone (4): Sulfuric acid was slowly added to lapachol (**1**) (1 mmol, 242 mg) until complete dissolution of the quinone. Then, the solution was poured into ice and the precipitate formed was filtered and washed with water. β -Lapachone (**4**) was recrystallized in an appropriate solvent, as for instance, ethanol. Compound **4** was obtained as an orange solid (240 mg, 99% yield); m.p. 153-155 °C. ^1H NMR (400 MHz, CDCl_3 , 303 K) δ : 8.06 (dd, 1H, $J = 7.6$ and 1.4 Hz), 7.81 (dd, 1H, $J = 7.8$ and 1.1 Hz), 7.65 (ddd, 1H, $J = 7.8, 7.6$ and 1.4 Hz), 7.51 (td, 1H, $J = 7.6, 7.6$ and 1.1 Hz), 2.57 (t, 2H, $J = 6.7$ Hz), 1.86 (t, 2H, $J = 6.7$ Hz),

1.47 (s, 6H). ^{13}C NMR (100 MHz, CDCl_3 , 303 K) δ : 179.8, 178.5, 162.0, 134.7, 132.6, 130.6, 130.1, 128.5, 124.0, 112.7, 79.3, 31.6, 26.8, 16.2. Data are consistent with those reported in the literature.^{48,49}

General Procedure for the Syntheses of P1 and the iodinated derivative 5

(Oxazole Formation):^{39,50} To a solution of 3-azide-nor- β -lapachone (**3**) (1.0 mmol) or β -lapachone (**4**) (242 mg, 1 mmol) in acetic acid (10 mL), salicylaldehyde (244 mg, 0.2 mL, 2.0 mmol) or 2-hydroxy-3,5-diodobenzaldehyde (561 mg, 1.5 mmol) was added, and the mixture was heated to 70 °C; at this point, ammonium acetate (1.54 g, 20 mmol) was slowly added, and the temperature was maintained at 110 °C. All the reactions were monitored by thin layer chromatography and it was observed that after four hours all the starting material was consumed. At this point, the reaction was cooled to room temperature and extracted with dichloromethane and dried with Na_2SO_4 . The solvent was removed under reduced pressure to afford the crude product, which was purified on a silica column using a gradient mixture of hexane/ethyl acetate as eluent (1% of ethyl acetate in hexane).

Compound **P1** was obtained as a white solid (196 mg, 0.7 mmol, 72% yield); m.p. 169-170 °C. ^1H NMR (400 MHz, CDCl_3 , 303 K) δ : 1.58 (s, 3H), 1.73 (s, 3H), 5.13 (s, 1H), 7.03 (ddd, 1H, $J = 7.9, 7.3$ and 1.1 Hz), 7.15 (ddd, 1H, $J = 8.3, 1.1$ and 0.4 Hz), 7.42 (ddd, 1H, $J = 8.3, 7.3$ and 1.7 Hz), 8.06 (ddd, 1H, $J = 7.9, 1.7$ and 0.4 Hz), 7.55 (ddd, 1H, $J = 8.3, 7.0$ and 1.2 Hz), 7.71 (ddd, 1H, $J = 8.3, 7.0$ and 1.2 Hz), 8.11 (ddd, 1H, $J = 8.3, 1.2$ and 0.8 Hz), 8.44 (ddd, 1H, $J = 8.3, 1.2$ and 0.8 Hz), 11.38 (s, 1H). ^{13}C NMR (100 MHz, CDCl_3 , 303 K) δ : 22.3, 27.4, 69.4, 91.4, 102.7, 111.1, 117.3, 119.1, 119.7, 122.5, 123.4, 125.4, 126.5, 126.6, 128.6, 130.1, 132.7, 143.2, 155.5, 157.7, 160.6. EI/HRMS (m/z) $[\text{M}+\text{H}]^+$: 373.1285. Cald. for $[\text{C}_{21}\text{H}_{17}\text{N}_4\text{O}_3]^+$: 373.1300.

Compound **5** was obtained as a grey solid (378 mg, 0.76 mmol, 76% yield); m.p. 279-280 °C. ¹H NMR (400 MHz, CDCl₃, 303 K) δ: 1.43 (s, 6H), 1.95 (t, 2H, *J* = 6.6 Hz), 3.06 (t, 2H, *J* = 6.6 Hz), 7.43-7.49 (m, 1H), 7.53-7.60 (m, 1H), 8.05 (d, 1H, *J* = 2.1 Hz), 8.20 (d, 1H, *J* = 2.1 Hz), 8.21-8.26 (m, 2H). ¹³C NMR (100 MHz, CDCl₃, 303 K) δ: 17.4, 26.7, 31.6, 75.7, 81.0, 86.5, 101.6, 113.2, 121.6, 122.9, 124.3, 125.2, 127.2, 127.4, 134.4, 139.1, 146.9, 148.4, 149.0, 156.2, 157.7.

Click chemistry reaction for preparing **P2** was accomplished as previously classical procedure described by Sharpless with minor modifications.⁴⁰ Compound **P1** (136 mg, 0.5 mmol) was reacted with CuSO₄·5H₂O (0.04 mmol), sodium ascorbate (0.15 mmol) and 1-pentadecyne (217 mg, 0.28 mL, 1.0 mmol) in a mixture of CH₂Cl₂:H₂O (15 mL, 2:1, v/v). The mixture was stirred at room temperature, and the reaction was monitored by thin layer chromatography. The aqueous phase was extracted with CH₂Cl₂, dried over anhydrous Na₂SO₄ and concentrated under reduced pressure. The residue was purified by column chromatography on silica gel eluting with a gradient mixture of hexane:ethyl acetate. With 1% of ethyl acetate in hexane the product was eluted and isolated as a white solid. Compound **P2** was obtained as a white solid (162 mg, 0.38 mmol, 75% yield); m.p. 143-144 °C. ¹H NMR (400 MHz, CDCl₃, 303 K) δ: 0.87 (t, 3H *J* = 7.0 Hz), 1.10-1.33 (m, 23H), 1.55 (q, 2H, *J* = 7.4 Hz), 1.76 (s, 3H), 2.53-2.68 (m, 2H), 6.47 (s, 1H), 6.81 (s, 1H), 6.96 (ddd, 1H, *J* = 7.9, 1.7 and 0.4 Hz), 7.11 (ddd, 1H, *J* = 8.3, 1.1 and 0.4 Hz), 7.39 (ddd, 1H, *J* = 8.3, 7.2 and 1.7 Hz), 7.62 (ddd, 1H, *J* = 8.3, 7.0 and 1.2 Hz), 7.78 (ddd, 1H, *J* = 8.3, 7.0 and 1.2 Hz), 7.87 (ddd, 1H, *J* = 7.9, 1.7 and 0.4 Hz), 8.19 (ddd, 1H, *J* = 8.3, 1.2 and 0.8 Hz), 8.48 (ddd, 1H, *J* = 8.3, 1.2 and 0.8 Hz), 11.31 (s, 1H). ¹³C NMR (100 MHz, CDCl₃, 303 K) δ: 14.1, 21.7, 22.7, 25.7, 27.3, 29.1, 29.2, 29.3, 29.4(6), 29.5(5), 29.5(8), 29.6(1), 29.6(4), 31.9, 68.1, 91.9, 117.2, 101.3, 110.7, 119.1, 119.7, 119.9, 122.6, 123.5, 125.8, 126.6, 126.9, 129.1,

130.6, 132.9, 142.6, 148.8, 156.1, 157.7, 160.9. Two ^{13}C resonances were observed at 29.2, as confirmed by HSQC analysis. Some of the ^{13}C chemical shifts were indicated with two decimals in order to differentiate nuclei with very similar resonance frequencies. EI/HRMS (m/z) $[\text{M}+\text{H}]^+$: 581.3501. Cald. for $[\text{C}_{36}\text{H}_{45}\text{N}_4\text{O}_3]^+$: 581.3491.

General Procedure for the Syntheses of P3 and P4 (Suzuki reaction): In a Schlenk tube was added iodinated oxazole **5** (239 mg, 0.4 mmol), phenylboronic acid (1.0 mmol), palladium(II) acetate (3 mg, 0.01 mmol), triphenylphosphine (11 mg, 0.04 mmol) sodium carbonate (350 mg, 3.2 mmol), 2 mL of water, 1 mL of methanol and 12 mL of toluene. The Schlenk tube was sealed and heated to 70 °C for 36 hours. The reaction was cooled to room temperature and the solvent was evaporated under reduced pressure. The product was extracted with dichloromethane and dried with Na_2SO_4 . The solvent was removed under reduced pressure to afford the crude product, which was purified on a silica column using a gradient mixture of hexane/ethyl acetate as eluent (1% of ethyl acetate in hexane).

Compound **P3** was obtained as a yellow solid (160 mg, 0.30 mmol, 80% yield); m.p. 247-248 °C. ^1H NMR (400 MHz, CDCl_3 , 303 K) δ : 1.49 (s, 6H), 2.01 (t, 2H, $J = 6.6$ Hz), 3.14 (t, 2H, $J = 6.6$ Hz), 7.44-7.53 (m, 5H), 7.60 (ddd, 1H, $J = 8.3$, 6.9 and 1.2 Hz), 7.66-7.69 (m, 2H), 7.72-7.76 (m, 2H), 8.23 (d, 1H, $J = 2.4$ Hz), 8.30 (dd, 2H, $J = 8.3$ and 1.1 Hz), 12.20 (s, 1H). ^{13}C NMR (100 MHz, CDCl_3 , 303 K) δ : 17.5, 26.8, 31.7, 75.5, 101.7, 112.1, 121.6, 122.8, 123.8, 124.2, 124.4, 124.9, 126.9, 127.1, 127.4, 127.5, 128.2, 128.9, 129.5, 130.6, 132.1, 132.7, 137.9, 140.4, 146.5, 148.4, 154.4, 160.4. Two ^{13}C resonances were observed at 127.1, as confirmed by HSQC analysis. EI/HRMS (m/z) $[\text{M}+\text{H}]^+$: 498.2063. Cald. for $[\text{C}_{34}\text{H}_{28}\text{NO}_3]^+$: 498.2069.

Compound **P4** was obtained as a yellow solid (100 mg, 0.18 mmol, 61% yield); m.p. 227-228 °C. ^1H NMR (400 MHz, CDCl_3 , 303 K) δ : 1.48 (s, 6H), 2.00 (t, 2H, $J =$

6.4 Hz), 3.13 (t, 2H, $J = 6.4$ Hz), 3.85 (s, 3H), 3.87 (s, 3H), 6.99 (d, 1H, $J = 8.7$ Hz), 7.03 (d, 1H, $J = 8.4$ Hz), 7.44-7.52 (m, 1H), 7.55-7.63 (m, 4H), 7.67 (d, 2H, $J = 8.4$ Hz), 8.12 (d, 1H, $J = 1.8$ Hz), 8.28 (d, 1H, $J = 8.6$ Hz), 12.11 (s, 1H). ^{13}C NMR (100 MHz, CDCl_3 , 303 K) δ : 17.5, 26.8, 31.7, 55.4, 75.5, 101.7, 111.9, 113.7, 114.3, 121.6, 122.8, 122.9, 124.1, 124.4, 124.8, 127.0, 127.5, 127.9, 130.1, 130.3, 130.6, 131.6, 132.4, 133.1, 146.4, 148.3, 159.0, 159.1, 153.9, 160.6. EI/HRMS (m/z) $[\text{M}+\text{H}]^+$: 558.2285
Cald. for $[\text{C}_{36}\text{H}_{32}\text{NO}_5]^+$: 558.2280.

ASSOCIATED CONTENT

1D and 2D NMR spectra, HRMS [ESI(+)-MS], photophysical analyses, cellular experimental procedures and Cartesian coordinates for the calculated structures, and energy and thermal corrections. The Supporting Information is available free of charge at DOI: xxxxx.

ACKNOWLEDGMENTS

This research was funded by grants from CNPq (PVE 401193/2014-4), FAPEMIG (Edital 01/2014 (APQ-02478-14) and Programa Pesquisador Mineiro – PPM X), CAPES, FAPDF, FINATEC, DPP-UnB, INCT-Transcend group and CAPES/PROCAD.

REFERENCES

1. A. Nadler and C. Schultz, *Angew. Chem., Int. Ed.*, 2013, **52**, 2408-2410.
2. K. Kikuchi, *Chem. Soc. Rev.*, 2010, **39**, 2048-2053.
3. J. Liang, B. Z. Tang and B. Liu, *Chem. Soc. Rev.*, 2015, **44**, 2798-2811.
4. D. Ding, K. Li, B. Liu and B. Z. Tang, *Acc. Chem. Res.*, 2013, **46**, 2441-2453.
5. L. D. Lavis and R. T. Raines, *ACS Chem. Biol.*, 2014, **9**, 855-866.
6. S. H. Alamudi, R. Satapathy, J. Kim, D. Su, H. Ren, R. Das, L. Hu, E. Alvarado-Martinez, J. Y. Lee, C. Hoppmann, E. Pena-Cabrera, H.-H. Ha, H.-S. Park, L. Wang and Y.-T. Chang, *Nat. Commun.*, 2016, **7**, 11964.

7. B. A. D. Neto, P. H. P. R. Carvalho and J. R. Correa, *Acc. Chem. Res.*, 2015, **48**, 1560-1569.
8. B. A. D. Neto, A. A. M. Lapis, E. N. da Silva Júnior and J. Dupont, *Eur. J. Org. Chem.*, 2013, 228-255.
9. B. A. D. Neto, J. R. Correa and R. G. Silva, *RSC Adv.*, 2013, **3**, 5291-5301.
10. Y. Kim, M. Choi, S. Seo, S. T. Manjare, S. Jon and D. G. Churchill, *RSC Adv.*, 2014, **4**, 64183-64186.
11. S. Goswami, S. Das, K. Aich, B. Pakhira, S. Panja, S. K. Mukherjee and S. Sarkar, *Org. Lett.*, 2013, **15**, 5412-5415.
12. A. K. Mahapatra, K. Maiti, S. K. Manna, R. Maji, C. Das Mukhopadhyay, B. Pakhira and S. Sarkar, *Chem.-Asian J.*, 2014, **9**, 3623-3632.
13. A. Paul, S. Anbu, G. Sharma, M. L. Kuznetsov, M. da Silva, B. Koch and A. J. L. Pombeiro, *Dalton Trans.*, 2015, **44**, 16953-16964.
14. M. Roy, B. Chakravarthi, C. Jayabaskaran, A. A. Karande and A. R. Chakravarty, *Dalton Trans.*, 2011, **40**, 4855-4864.
15. S. T. Nguyen, S. M. Kwasny, X. Y. Ding, J. D. Williams, N. P. Peet, T. L. Bowlin and T. J. Opperman, *Bioorg. Med. Chem.*, 2015, **23**, 5789-5798.
16. Y. C. Hao, M. L. Zheng and Y. Chen, *J. Mater. Chem. B*, 2014, **2**, 7369-7374.
17. Q. Wang, L. Zhou, L. Qiu, D. Lu, Y. Wu and X.-B. Zhang, *Analyst*, 2015, **140**, 5563-5569.
18. C. Li, Y. Yang, C. Ma and Y. Liu, *RSC Adv.*, 2016, **6**, 5134-5140.
19. Y. Xu, L. Xiao, S. Sun, Z. Pei, Y. Pei and Y. Pang, *Chem. Commun.*, 2014, **50**, 7514-7516.
20. Y. Houari, A. Charaf-Eddin, A. D. Laurent, J. Massue, R. Ziessel, G. Ulrich and D. Jacquemin, *Phys. Chem. Chem. Phys.*, 2014, **16**, 1319-1321.
21. J. Massue, G. Ulrich and R. Ziessel, *Eur. J. Org. Chem.*, 2013, **2013**, 5701-5709.
22. R. F. Affeldt, R. S. Iglesias, F. S. Rodembusch and D. Russowsky, *J. Phys. Org. Chem.*, 2012, **25**, 769-777.
23. K. Benelhadj, W. Muzuzu, J. Massue, P. Retailleau, A. Charaf-Eddin, A. D. Laurent, D. Jacquemin, G. Ulrich and R. Ziessel, *Chem.-Eur. J.*, 2014, **20**, 12843-12857.
24. P. F. Dick, F. L. Coelho, F. S. Rodembusch and L. F. Campo, *Tetrahedron Lett.*, 2014, **55**, 3024-3029.
25. J. E. Kwon, S. Lee, Y. You, K. H. Baek, K. Ohkubo, J. Cho, S. Fukuzumi, I. Shin, S. Y. Park and W. Nam, *Inorg. Chem.*, 2012, **51**, 8760-8774.
26. V. S. Patil, V. S. Padalkar, A. B. Tathe, V. D. Gupta and N. Sekar, *J. Fluoresc.*, 2013, **23**, 1019-1029.
27. S. T. A. Passos, J. R. Correa, S. L. M. Soares, W. A. da Silva and B. A. D. Neto, *J. Org. Chem.*, 2016, **81**, 2646-2651.
28. A. A. R. Mota, J. R. Corrêa, P. H. P. R. Carvalho, N. M. P. de Sousa, H. C. B. de Oliveira, C. C. Gatto, D. A. da Silva Filho, A. L. de Oliveira and B. A. D. Neto, *J. Org. Chem.*, 2016, **81**, 2958-2965.
29. C. D'Angelis do E. S. Barbosa, J. R. Corrêa, G. A. Medeiros, G. Barreto, K. G. Magalhães, A. L. de Oliveira, J. Spencer, M. O. Rodrigues and B. A. D. Neto, *Chem. -Eur. J.*, 2015, **21**, 5055-5060.
30. G. G. Dias, B. L. Rodrigues, J. M. Resende, H. D. R. Calado, C. A. de Simone, V. H. C. Silva, B. A. D. Neto, M. O. F. Goulart, F. R. Ferreira, A. S. Meira, C. Pessoa, J. R. Correa and E. N. da Silva Júnior, *Chem. Commun.*, 2015, **51**, 9141-9144.
31. P. H. P. R. Carvalho, J. R. Correa, B. C. Guido, C. C. Gatto, H. C. B. De Oliveira, T. A. Soares and B. A. D. Neto, *Chem.-Eur. J.*, 2014, **20**, 15360-15374.
32. J. R. Diniz, J. R. Correa, D. D. Moreira, R. S. Fontenele, A. L. de Oliveira, P. V. Abdelnur, J. D. L. Dutra, R. O. Freire, M. O. Rodrigues and B. A. D. Neto, *Inorg. Chem.*, 2013, **52**, 10199-10205.
33. S. L. de Castro, F. S. Emery and E. N. da Silva Júnior, *Eur. J. Med. Chem.*, 2013, **69**, 678-700.

34. E. N. da Silva Júnior, G. A. M. Jardim, R. F. S. Menna-Barreto and S. L. de Castro, *J. Braz. Chem. Soc.*, 2014, **25**, 1780-1798.
35. G. A. M. Jardim, W. J. Reis, M. F. Ribeiro, F. M. Ottoni, R. J. Alves, T. L. Silva, M. O. F. Goulart, A. L. Braga, R. F. S. Menna-Barreto, K. Salomao, S. L. de Castro and E. N. da Silva Júnior, *RSC Adv.*, 2015, **5**, 78047-78060.
36. E. H. G. da Cruz, M. A. Silvers, G. A. M. Jardim, J. M. Resende, B. C. Cavalcanti, I. S. Bomfim, C. Pessoa, C. A. de Simone, G. V. Botteselle, A. L. Braga, D. K. Nair, I. N. N. Namboothiri, D. A. Boothman and E. N. da Silva Júnior, *Eur. J. Med. Chem.*, 2016, **122**, 1-16.
37. G. A. M. Jardim, H. D. R. Calado, L. A. Cury and E. N. da Silva Júnior, *Eur. J. Org. Chem.*, 2015, 703-709.
38. L. F. Fieser and M. Fieser, *J. Am. Chem. Soc.*, 1948, **70**, 3215-3222.
39. C. N. Pinto, A. P. Dantas, K. C. G. De Moura, F. S. Emery, P. F. Polequevitch, M. D. Pinto, S. L. de Castro and A. V. Pinto, *Arzneimittelforschung-Drug Res.*, 2000, **50**, 1120-1128.
40. H. C. Kolb, M. G. Finn and K. B. Sharpless, *Angew. Chem., Int. Ed.*, 2001, **40**, 2004-2021.
41. C. W. Tornøe, C. Christensen and M. Meldal, *J. Org. Chem.*, 2002, **67**, 3057-3064.
42. M. Meldal and C. W. Tornøe, *Chem. Rev.*, 2008, **108**, 2952-3015.
43. B. K. Paul, A. Samanta and N. Guchhait, *J. Fluoresc.*, 2011, **21**, 1265-1279.
44. D. R. da Rocha, K. Mota, I. M. C. B. da Silva, V. F. Ferreira, S. B. Ferreira and F. C. da Silva, *Tetrahedron*, 2014, **70**, 3266-3270.
45. M. Niehues, V. P. Barros, F. S. Emery, M. Dias-Baruffi, M. d. D. Assis and N. P. Lopes, *Eur. J. Med. Chem.*, 2012, **54**, 804-812.
46. E. P. Sacau, A. Estevez-Braun, A. G. Ravelo, E. A. Ferro, H. Tokuda, T. Mukainaka and H. Nishino, *Bioorg. Med. Chem.*, 2003, **11**, 483-488.
47. E. N. da Silva Júnior, R. F. S. Menna-Barreto, M. Pinto, R. S. F. Silva, D. V. Teixeira, M. de Souza, C. A. De Simone, S. L. De Castro, V. F. Ferreira and A. V. Pinto, *Eur. J. Med. Chem.*, 2008, **43**, 1774-1780.
48. S. C. Hooker, *J. Am. Chem. Soc.*, 1936, **58**, 1190-1197.
49. K. Schaffnersabba, K. H. Schmidtrupp, W. Wehrl, A. R. Schuerch and J. W. F. Wasley, *J. Med. Chem.*, 1984, **27**, 990-994.
50. K. C. G. De Moura, F. S. Emery, C. Neves-Pinto, M. Pinto, A. P. Dantas, K. Salomao, S. L. de Castro and A. V. Pinto, *J. Braz. Chem. Soc.*, 2001, **12**, 325-338.